



ENTIRE-SPRAY MIXING CHARACTERISTICS OVER TIME AFTER THE START OF THE INJECTION USING AN IMAGE-PROCESSING TECHNIQUE FOR HIGH-SPEED CAPTURED IMAGES OF CR-DI FUEL SPRAYS

Choong Hoon Lee

Department of Mechanical and Automotive Engineering, Seoul National University of Science and Technology, Seoul, Korea

E-Mail: chlee5@seoultech.ac.kr

ABSTRACT

Diesel fuel sprays from a common rail injector were injected into a pressurized constant-volume chamber. The environmental gas density in the constant-volume chamber was 18 kg/m^3 , which is representative of the density in a typical diesel engine when the fuel injection process starts. Consecutive images of the diesel fuel sprays were captured with a high-speed camera at a constant time interval. The spray dispersion area with time after the start of the fuel injection was obtained. The spray dispersion area increased linearly with time after the start of the injection. The slope of the linear correlation line between the spray dispersion area and time after the start of the injection was steeper when the fuel injection pressure was higher. There was little effect on the slope of the linear correlation line with a change of the duration of the fuel injection time. The mixing characteristics of the entire spray injected from the common rail diesel injector were studied by analyzing the capture images. The mixing characteristics of all sprays over time after the start of the injection process were quantified by determining the pure-light-extinction intensity (PLEI) at each pixel for all of the sprays.

Keywords: spray mixing characteristics, light-extinction intensity, edge detection, diesel spray, image processing.

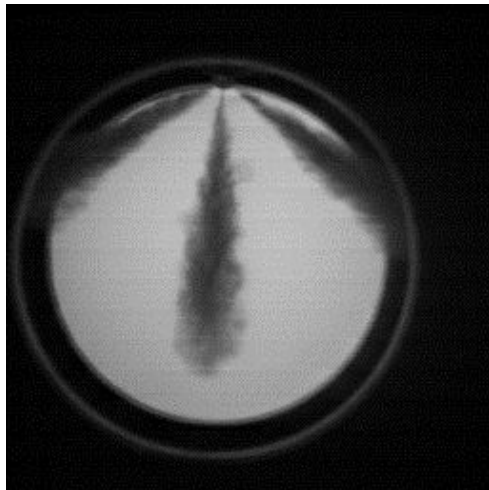
INTRODUCTION

With the introduction of various advanced technologies, the performance of diesel engines has been continuously improved [1-3]. In particular, diesel engine performance levels have been dramatically improved by changing the fuel injection control from a mechanical system to an electronically controlled fuel injection system using a common rail. With the common rail system and electronically controlled injectors, a constant fuel pressure can be maintained while injecting fuel from the injector, and the fuel injection timing can be freely controlled. The mechanical injection system undergoes a large change in the pressure during the injection of the fuel and restriction of the injection timing. The average fuel injection pressure in the fuel injection process of the diesel common rail system is approximately four times that of a mechanical fuel injection system [4-6]. In addition, the common rail injector is controlled electronically, implying that multiple injection types, including pilot injection, are possible and that the control of the injection timing is very accurate. Pilot injection controlled at a precise injection timing can drastically reduce NO_x, noise and vibration in diesel engines by precisely controlling the amount of the pre-mixture formed in the combustion chamber of the diesel engine. The effects of a multiple-injection scheme on diesel engine performance outcomes have been assessed by many researchers [7-11].

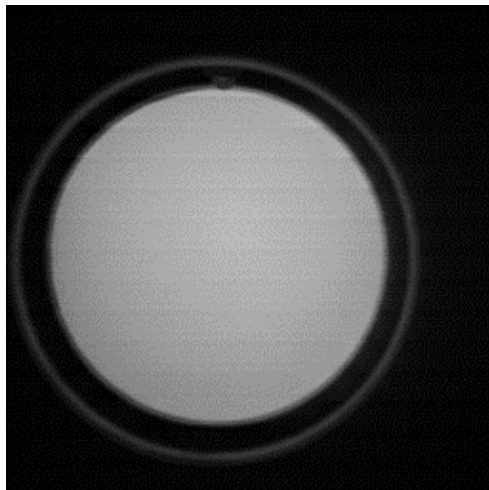
The key to improving diesel engine performance is rapid air-fuel mixing in the combustion chamber. The most important factor affecting the mixing of the diesel fuel and air is the injection pressure of the fuel. In general, increasing the injection pressure of the fuel promotes air-fuel mixing. Air-fuel mixing is promoted by increasing the fuel injection pressure because a faster spray jet with a higher injection pressure promotes atomization. In

addition, when the fuel injection pressure is high, the injector nozzle hole size can be reduced, which promotes the atomization of the fuel jet. The swirl flow induced by the intake port in the engine cylinder head affects the air-fuel mixing characteristics. The swirl flow in the combustion chamber deflects the spray in a tangential direction, thereby promoting air-fuel mixing. The shape of the combustion chamber also affects the air-fuel mixing. Lee [12] studied the dispersion characteristics of diesel sprays with swirl flows using a visualization method. In addition, Hiroyasu *et al.* [13,14] and Klein-Douwelle [15] assessed the dispersion characteristics of diesel sprays experimentally. In a diesel engine, when the piston approaches the top dead center, highly pressurized fuel is injected and a squish flow is formed by the gap between the piston and the cylinder head. This squish flow pattern is affected by the shape of the combustion chamber and consequently influences the air-fuel mixing.

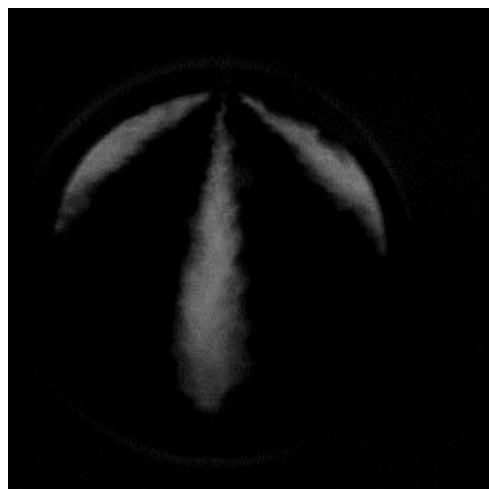
For the above reasons, it is very important to understand the distribution of the air-fuel mix in the combustion chamber of the diesel spray under various injection conditions to improve the diesel engine performance. Zhang *et al.* [16], Gao *et al.* [17] and Chengjun *et al.* [18] studied the mixing characteristics of diesel sprays using the laser absorption scattering (LAS) technique. Felton *et al.* [19] studied the mixing characteristics of diesel sprays using a laser-induced exciplex fluorescence (LIEF) method. Rabenstein *et al.* [20] researched the mixing characteristics using the Raman scattering method. Nawi *et al.* [21] studied the diesel spray mixing characteristics using a shadowgraph method.



(a)



(b)



(c)

Figure-1. Image subtraction to obtain the PLEI (pure light-extinction intensity): (a) original captured image, (b) background image, and (c) subtracted image.

Meanwhile, there is a lack of research on the distribution of the air-fuel mix of an entire diesel spray

over time after the start of the fuel injection. In this study, diesel fuel from a common rail injector is injected into a static spray chamber. Consecutive images of the diesel fuel sprays were captured with a high-speed camera at a constant time interval. The characteristics of air-fuel mixing of the entire spray with time after the start of the fuel injection were investigated using an image-processing technique.

EXPERIMENTS

Experimental data from Tennison *et al.* [22] was used in this study. Tennison *et al.* injected fuel with multiple injections, in that case single, pilot, and split patterns and visualized diesel spray images using a pulsed copper vapor laser, a high-speed camera and an optical system arrangement. The experiment by Tennison *et al.* can be summarized as follows.

The fuel injection system used consisted of a fuel tank, a low-pressure pump, a high-pressure pump and a common rail accumulator. The injector used was a solenoid-type common rail injector. The injection timing and quantity are controlled by the ECU by changing the timing and duration. The injector nozzle tip diameter was 0.16 mm. There were six holes. The hole length was 1.0 mm and the L/D ratio was 6.25. The injection spray angle was 145°.

The visualization system of the diesel fuel spray consisted of a laser light source, various lenses and mirrors, a see-through high-pressure spray chamber, and a high-speed digital camera. The laser light source was a pulsed copper-vapor laser with wavelengths of 510.6 nm (green) and 578.2 nm (yellow). The duration of each laser pulse is 10~40 ns and the average energy per pulse is 2 mJ. The spray chamber is a metal cylinder that provides an environment of high-pressure (density) gas at room temperature. Optical-grade quartz windows are mounted to end plates at each end of the cylinder, providing see-through access. The injector was mounted through one of the endplates at a 72.5° angle to allow one of the spray angles of the 145° angled nozzle to be perpendicular to the light beam path. Most of the data in the experiment were taken at a frame rate of 4500 frames/sec.

RESULTS AND DISCUSSIONS

The light-extinction images of the diesel fuel sprays were captured with a time interval of 0.22 ms. The digital format of the image contains 256x256 pixels. In order to obtain the pure light-extinction intensity (PLEI) on the high-speed captured image, the background image shown in Figure-1b was subtracted from the original captured image shown in Figure-1a. The PLEI distribution of the subtracted image was digitized with a gray-scale resolution of 256 levels. The PLEI with a higher value at a pixel in the subtracted image means a higher fuel concentration from the perspective of air-fuel mixing. The twelfth frame from the start of the fuel injection was applied to the subtraction process as an example. The image in Figure-1(c) is the subtract

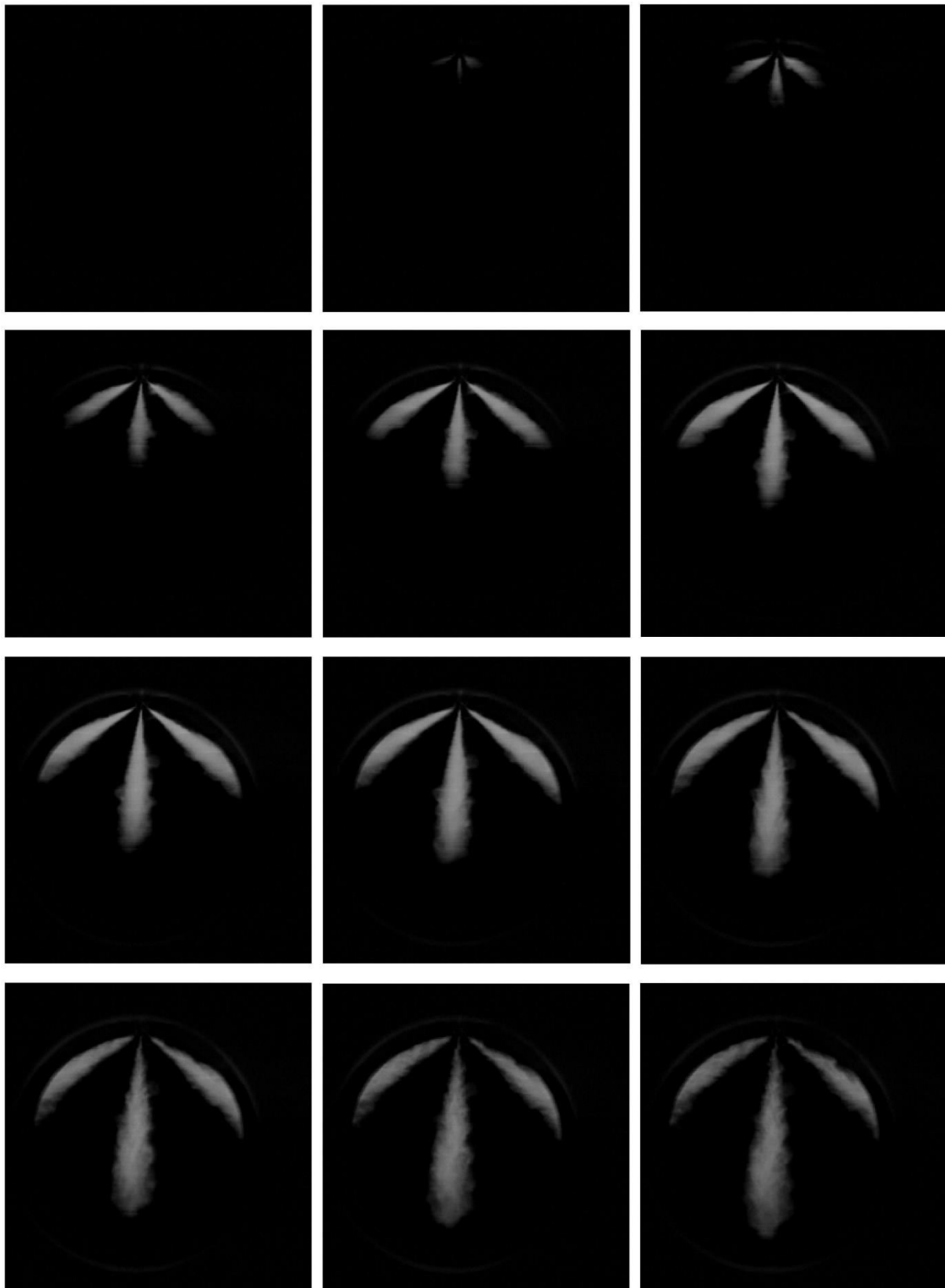


Figure-2. Consecutive subtracted image at a time interval of 0.22 ms.

result. Figure-2 shows consecutively subtracted images at a time interval of 0.22 ms which were obtained by applying an earlier image-processing technique for diesel sprays. The fuel injection pressure and duration of the

diesel spray shown in Figure-2 are 900 bar and 1.0 ms, respectively. The subtracted images are displayed in the order of the captured time from the initial image at the left



and top to the final image at the right and bottom consecutively.

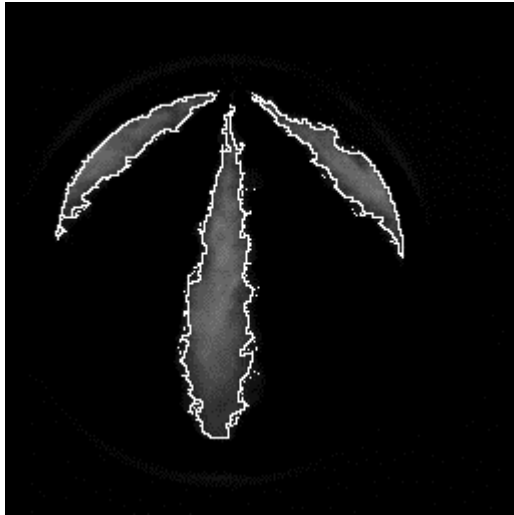


Figure-3. Edge detection results of a subtracted image.

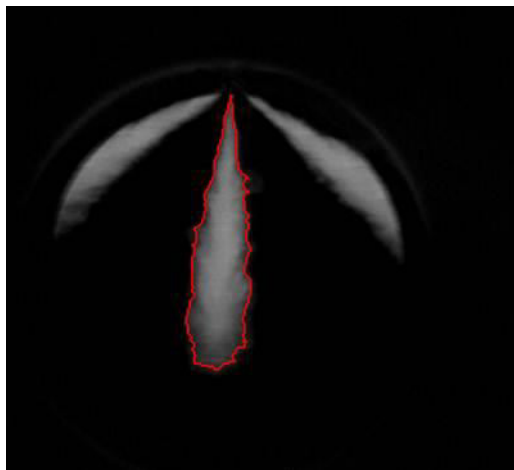


Figure-4. An example of edge detection results for the center spray plume.

Figure-3 shows the edge detection results of the subtracted image. The detection of the spray edge was performed using the NI-Vision Assistant® image-processing program in conjunction with an edge-detection technique. After the 'Measure' menu is executed in the NI-Vision7.0® IDE (integrated development environment), the measurement 'area' is selected. Then, the tolerance is set with the value of the maximum allowable deviation from the origin. All pixels satisfying the tolerance criteria ($\text{origin pixel} - \text{tolerance} / \text{origin pixel} + \text{tolerance}$) become part of the area. In the next step, clicking the 'Magic wand tool' button creates an image mask by extracting the region surrounding a reference pixel and using the tolerance of the intensity variations based on this reference pixel. The program searches for its boundaries with an intensity level equal to the tolerance value of the reference level or falling within an acceptable tolerance range.

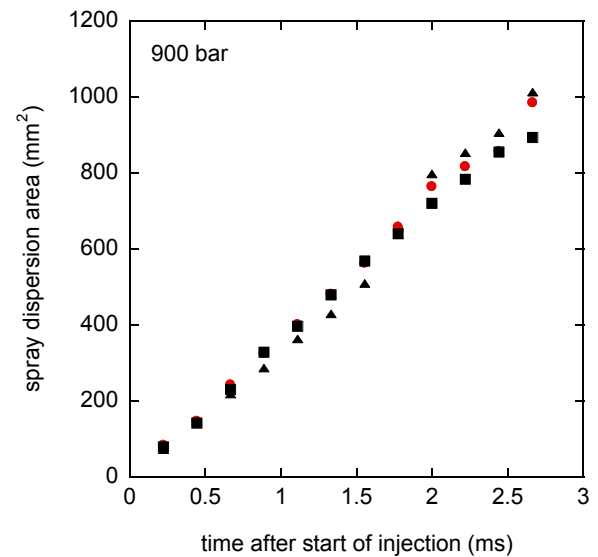


Figure-5. Spray dispersion area with time after the start of the fuel injection under the experimental conditions of a fuel injection pressure of 900 bar and injection durations of 1 ms and 1.5 ms.

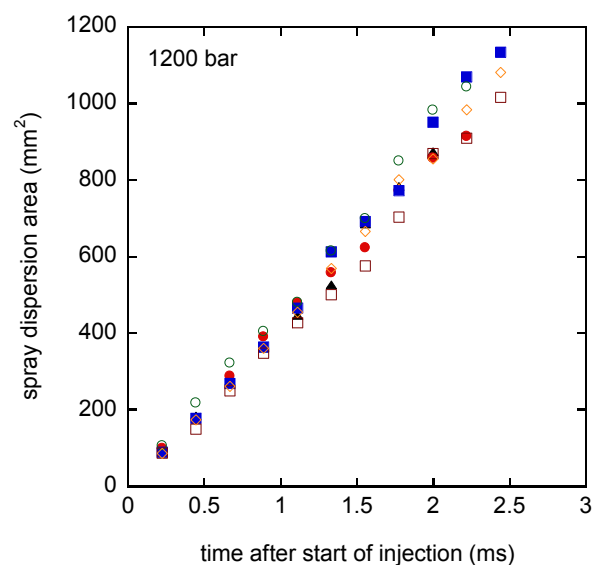


Figure-6. Spray dispersion area with time after the start of the fuel injection under the experimental conditions of a fuel injection pressure of 1200 bar and injection durations of 1 ms and 1.5 ms.

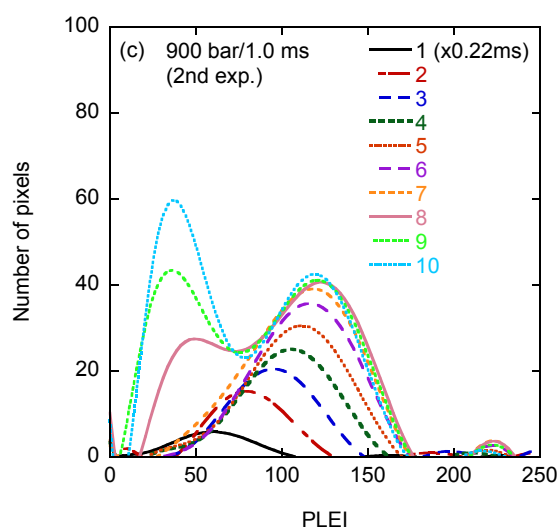
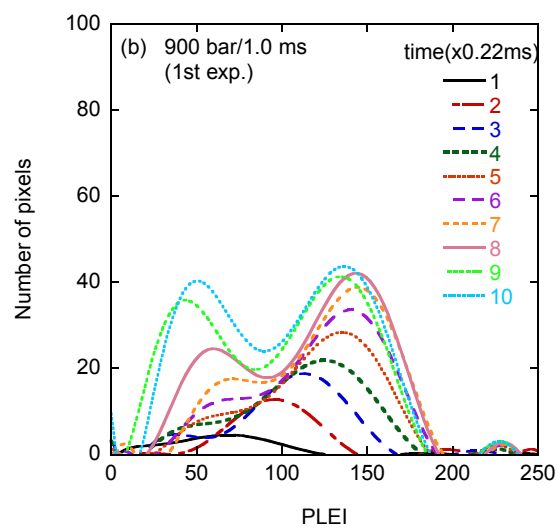
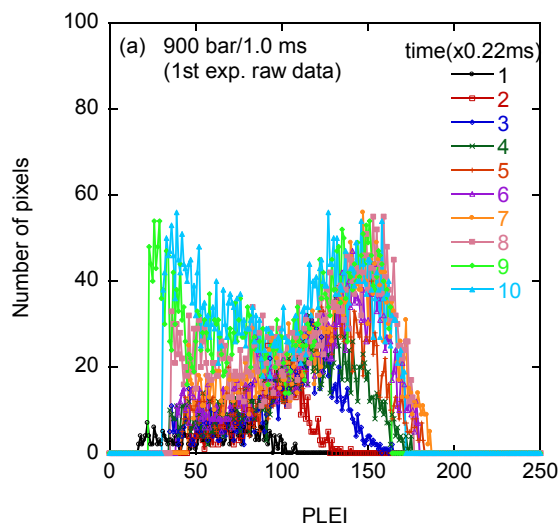


Figure-7. Number of pixel curves with the PLEI at an injection pressure of 900 bar and injection duration of 1.0 ms: (a) raw data (b) curve fitting of (a), and (c) second experiments.

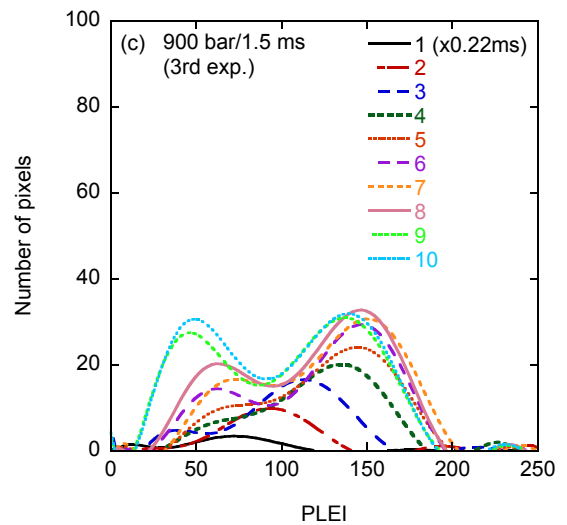
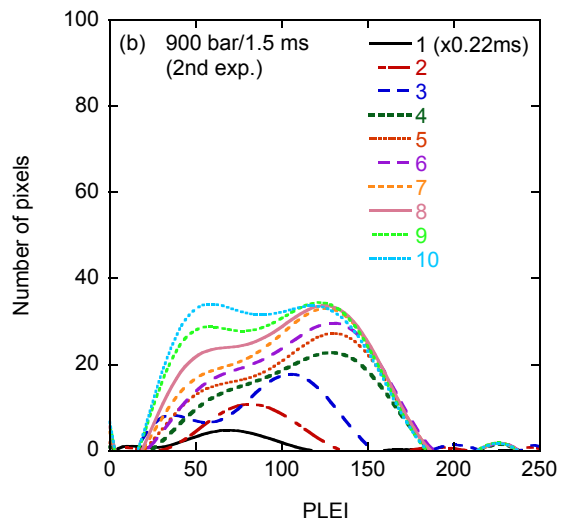
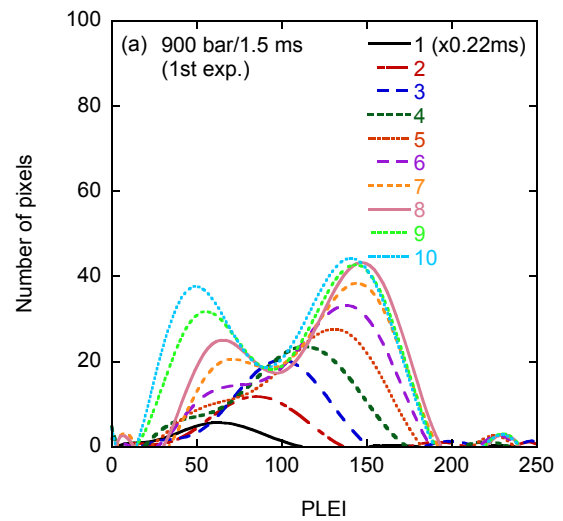


Figure-8. Number of pixel curves with the PLEI at an injection pressure of 900 bar and injection duration of 1.5 ms: (a) first experiment, (b) second experiment, and (c) third experiment.



In Figure-3, the center spray plume is perpendicular to the light beam path. The spray plumes on both sides of the center spray plume are not perpendicular to the light beam path. Figure-4 shows the edge detection results for the center spray plume. In this study, the dispersion area and PLEI of the center spray plume were analyzed. The dispersion area in the edge-detect boundary of the center spray plume was obtained, as was the PLEI of each pixel within the edge-detect boundary.

The spray dispersion area with time after the start of the fuel injection was obtained at an injection pressure of 900 bar. The spray dispersion area was determined using the spray edge-detection technique for each captured frame image with a time interval of 0.22 ms. Figure-5 shows the spray dispersion area with time after the start of the fuel injection. The fuel injection pressure and duration are 900 bar and 1.0ms/1.5ms, respectively. The fuel injection was repeated twice for 1.0 ms and three times for 1.5 ms. The spray dispersion area generally increases linearly with time after the start of the fuel injection.

A similar analysis of the spray dispersion area with time after the start of the fuel injection was performed at a fuel injection pressure of 1200 bar. Figure-6 shows the spray dispersion area with time after the start of the fuel injection. The fuel injection at 1200 bar was repeated three times for injection durations of 1.0 and 1.5 ms. The spray dispersion area also increases linearly with time after the start of the fuel injection, similar to the results at the fuel pressure of 900 bar except for the fact that the slope of the linear curve at 1200 bar is steeper than that at 900 bar.

Figure-7(a) shows the entire spray PLEI at 0.22 ms intervals when injecting the fuel at the pressure of 900 bar with a fuel injection duration of 1.0 ms. The number of pixels with a particular PLEI value indicates the size of the area occupied by the spray with a particular air-fuel mixture concentration. Figure-7(a) shows the change in the number of pixels according to the PLEI value (x-axis) using the raw experimental data. For an effective analysis, the pixel number curve with the PLEI at each time step was fitted with a polynomial curve. The results of curve fitting for Figure-7(a) are shown in Figure-7(b). The results of all subsequent are shown with the curve fitting.

The PLEI value ranged from 0 to 120 at 0.22 ms after the start of the fuel injection, and the maximum number of pixels was 5 at the PLEI value of 60. At each time step after the start of the fuel injection, the PLEI value increased to 190, and the minimum PLEI value was close to 10. The pixel number curve for the PLEI change at each time step shows one peak up to 1.32 ms (6x0.22 ms) after the start of the fuel injection. After the time step of 1.54 ms (7x0.22 ms), two peaks appeared in the pixel number curve. In the pixel number curve which has only one peak, the left lines which are located to the left with reference to the peak nearly merged into a line, while on the other hand, the space between the lines located to the right with reference to the peak increases evenly. After the time step when two peaks start to appear in the pixel number curve, the space between the right peak curves which appear at higher PLEI values

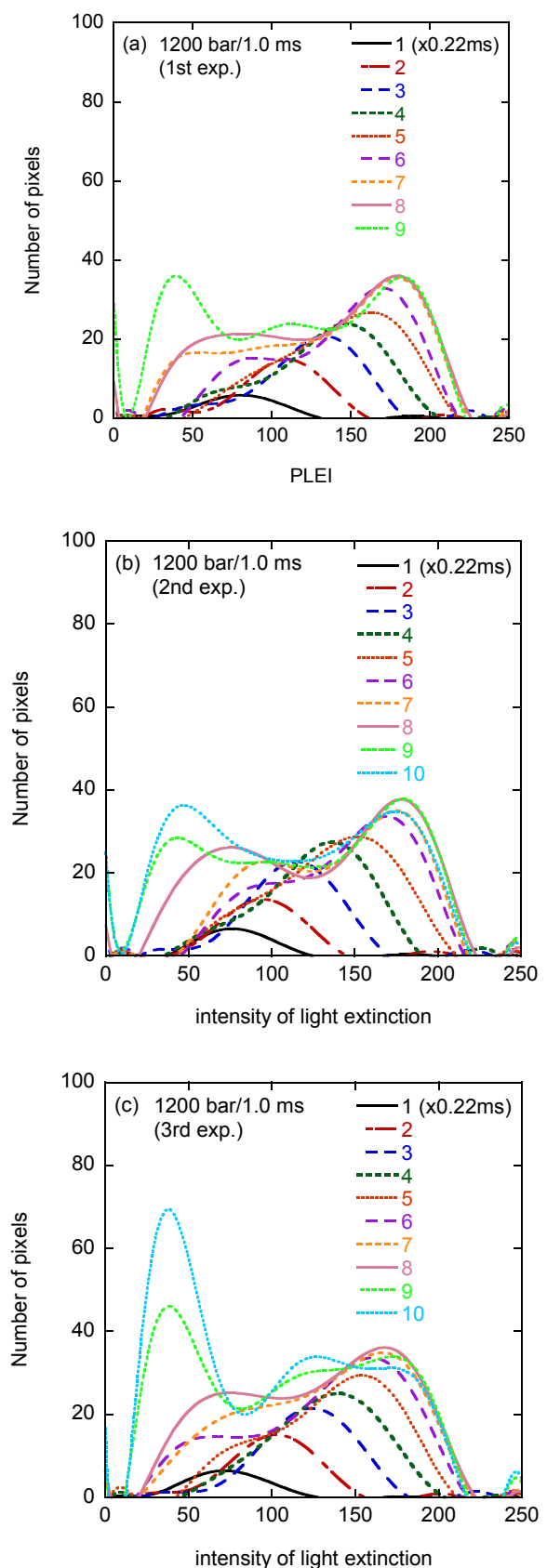


Figure-9. Number of pixel curves with the PLEI at an injection pressure of 1200 bar and injection duration of 1.0 ms: (a) first experiment, (b) second experiment, and (c) third experiment.



decreases and the right peak curves begins to converge into one curve. At the same time, a new peak starts to appear on the left. As the time step increases after the left peak appears, the space between the left curves is sufficiently large. In the time step when two peaks appear for the first time in the pixel number curve, the left peak is located near a PLEI value of 50 and the right peak is located near 150. In the pixel number curve at 2.2 ms (10×0.22 ms) after the start of the injection, the number of pixels was close to 40 at the PLEI values of 50 and 150. A PLEI value 50 indicates a relatively lean air-fuel mixture compared to that at a PLEI value 150. These results mean that a relatively leaner air-fuel mixture appears at the end of the fuel injection. At the end of the fuel injection, the pixel number curve converges to a curve having two peaks and remains as it is. In other words, at the end of the fuel injection, the distribution of the air-fuel mixture concentration shows two peak curves with a symmetrical shape. Figure-7(c) shows the results obtained with experimental conditions identical to those in Figure-7(b). Except for the left peak value of the pixel number curve, which is larger than that in Figure-7(b), the results shown in Figure-7(c) are similar to those in Figure-7(b).

Figure-8 shows the results at the conditions of an injection pressure of 900 bar and injection duration of 1.5 ms. The experiments are repeated three times. The results shown in Figure-8 are similar to those in Figure-7. The only difference between the two results is that the time when two peaks appear in the pixel number curve is earlier in Figure-8.

Figure-9 and Figure-10 show the results obtained when the fuels are injected at both 1200 bar/1.0 ms and 1200 bar/1.5 ms, respectively. The experiments conducted to obtain the results shown in Figure-9 and Figure-10 were repeated three times with identical conditions in each case. The results shown in Figure-9 and Figure-10 are similar to those shown in Figure-7 and Figure-8. The difference between them was that the pixel number curve was distributed over a wider PLEI range when the fuel injection pressure was 1200 bar. At 1200 bar, the PLEI range of the pixel number curve is from 1 to 220. At the fuel injection pressure of 1200 bar, the time when the two peaks in the pixel number curve is sooner at an injection duration of 1.5 ms than that at 1.0 ms. These results indicate that the higher the fuel injection pressure, the wider distribution of the air-fuel mixture concentration.

CONCLUSIONS

a) At each time step after the start of the fuel injection, the number of pixels which have a specific value of the PLEI was obtained through image processing for the entire spray. At an early time step after the start of the fuel injection, the pixel number curve shows one peak, whereas after a certain time step, two peaks appear as a symmetrical shape. This indicates that the concentration distribution curve of the air-fuel mixture for the entire spray has the shape of symmetrical two peaks, one lean and the other rich.

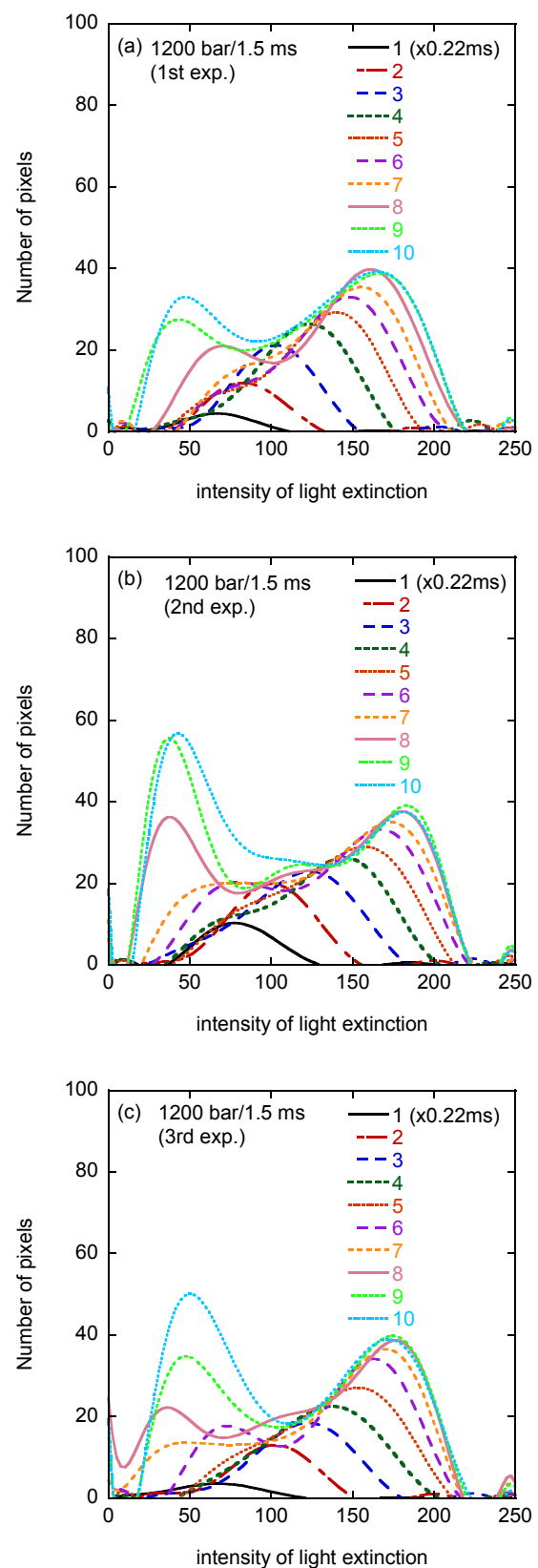


Figure-10. Number of pixel curves with the PLEI at an injection pressure of 1200 bar and injection duration of 1.5 ms: (a) first experiment, (b) second experiment, and (c) third experiment.



b) The time when two peaks appear in the pixel number curve was earlier at the fuel injection duration of 1.5 ms as compared to 1.0 ms.

c) The higher the fuel injection pressure, the wider the pixel number curve became, and the value of the pixel number curve increased over each time step. These results indicate that the higher the fuel injection pressure, the wider the distribution of the air-fuel mixture concentration.

ACKNOWLEDGEMENT

This study was supported by the research program funded by Seoul National University of Science and Technology. The author would like to thank Professor R. D. Reitz who allowed the author to use the experimental data for this research.

REFERENCES

- [1] F. E. Corcione, B. M. Vaglieco, G. E. Corcione, M. Lavorgna and R. Lanzafame. 2003. Study of the combustion system of a new small DI diesel engine with advanced common-rail injection system, SAE paper 2003-01-1858.
- [2] C. W. Park, S. H. Kook and C. S. Bae. 2004. Effects of multiple injections in a HSDI diesel engine equipped with common-rail injection system, SAE paper 2004-01-0029.
- [3] M. Besson, N. Hilaire, H. Lahjaily and P. Gastaldi. 2003. Diesel combustion study at full load using CFD and design of experiments, SAE paper 2003-01-1858.
- [4] Bosch. 2005. Diesel Engine Management. 4th edition, Robert Bosch GmbH.
- [5] Bosch Technical Instruction. 1996. Governors for Diesel In-Line Fuel-Injection Pumps. Edition 95/96, Robert Bosch GmbH.
- [6] Bosch Technical Instruction. 1983. Diesel Distributor Fuel-Injection Pumps, Edition 94/95, Robert Bosch GmbH.
- [7] Y. Hotta, M. Inayoshi, K. Nakakita, K. Fujiwara and I. Sakata. 2005. Achieving Lower Exhaust Emissions and Better Performance in an HSDI Diesel Engine with Multiple Injection, SAE paper No. 2005-01-0928.
- [8] M. Badami, F. Mallamo, F. Millo and E. E. Rossi. 2002. Influence of Multiple Injection Strategies on Emissions, Combustion Noise and BSFC of a DI Common Rail Diesel Engine, SAE Paper No. 2002-01-0503.
- [9] A. Kato, K. Matsuura, T. Hakozaki, O. Suzuki, S. Haraguchi, Y. Yoshimi, T. Katano, T. Hashimoto. 2011. Influence of a Fast Injection Rate Common Rail Injector for the Spray and Combustion Characteristics of Diesel Engine, SAE paper No. 2011-01-0687.
- [10] S. Shundoh, M. Komori, K. Tsujimura, S. Kobayashi. 1992. NOx Reduction from Diesel Combustion Using Pilot Injection with High Pressure Fuel Injection, SAE Technical Paper No. 920461.
- [11] T. Minami, K. Takeuchi and N. Shimazaki. 1995. Reduction of Diesel Engine NOx Using Pilot Injection, SAE Technical Paper No. 950611.
- [12] Lee C. H. 2013. An Experimental Study on the Correlation between Spray Dispersion Area and Tip Penetration Using an Edge Detection Technique of Images Captured from Highly Pressurized Cr-Di Fuel Injection. Advanced Materials Research. 787: 513-519.
- [13] Hiroyasu H. 1985. Diesel Engine Combustion and its Modeling, COMODIA85. 53-75.
- [14] Hiroyasu H., Kadota T. and Arai M. 1980. Supp. Comments: Fuel Spray Characterization in Diesel Engines, in J. N. Mattavi and C. A. Amann (eds.), Combustion Modeling in Reciprocating Engines, Plenum. 369-408.
- [15] R.J.H. Klein-Douwle, P.J.M. Frijters, L.M.T. Somers, W.A. de Boer and R.S.G. Baert. 2007. Macroscopic diesel fuel spray shadowgraphy using high speed digital imaging in a high pressure cell, Fuel. 86: 1994-2007.
- [16] Yuyin Zhang. 2014. Tomoaki Ito and Keiya Nishida Characterization of Mixture Formation in Split-Injection Diesel Sprays via Laser Absorption-Scattering (LAS) Technique 2001-01-3498.
- [17] Jian Gao, Keiya Nishida, Seoksu Moon and Yuhei Matsumoto, Characteristics of Evaporating Diesel Spray: A Comparison of Laser Measurements and Empirical/Theoretical Predictions
- [18] Chengjun Du, Mats Andersson and Sven Andersson. 2016. Effects of Nozzle Geometry on the Characteristics of an Evaporating Diesel Spray, 2016-01-2197.
- [19] Felton P. G., Bracco F. V. and Bardsley M. 1993. On the Quantitative Application of Exciplex Fluorescence



to Engine Sprays. SAE 1993 Transactions, Journal of Engines. paper 930870. 102 (3): 1254-1262.

- [20] Rabenstein F., Egermann J. and Leipertz A. 1998. Vapor-Phase Structure of Diesel-Type Fuel Sprays: An Experimental Analysis. SAE, Paper 982543, USA.
- [21] Mohd Al-Hafiz Mohd Nawawi, Naoya Uwa, Yuki Ueda, Yuzuru Nada and Yoshiyuki Kidoguchi. Droplets Behavior and Evaporation of Diesel Spray Affected by Ambient Density after Pilot Injection SAE 2015-32-0724.
- [22] Tennison P. J., Georjon T.L., Farrell P. V. and Reitz R. D. 1998. An Experimental and numerical study of sprays from a common rail injection system for use in an HSDI Diesel engine. SAE paper 980810.